Acta Cryst E CRYSTALLOGRAPHIC COMMUNICATIONS
ISSN 2056-9890

A 2:1 co-crystal of 2-methylbenzoic acid and *N*,*N*′-bis(pyridin-4-ylmethyl)ethanediamide: crystal structure and Hirshfeld surface analysis

Sabrina Syed,[a] Mukesh M. Jotani,[b]‡ Siti Nadiah Abdul Halim[a] and Edward R. T. Tiekink[c]*

[a]Department of Chemistry, University of Malaya, 50603 Kuala Lumpur, Malaysia, [b]Department of Physics, Bhavan's Sheth R. A. College of Science, Ahmedabad, Gujarat 380 001, India, and [c]Centre for Crystalline Materials, Faculty of Science and Technology, Sunway University, 47500 Bandar Sunway, Selangor Darul Ehsan, Malaysia. *Correspondence e-mail: edwardt@sunway.edu.my

Received 12 February 2016
Accepted 16 February 2016

Edited by W. T. A. Harrison, University of Aberdeen, Scotland

‡ Additional correspondence author, e-mail: mmjotani@rediffmail.com.

Keywords: crystal structure; co-crystal; hydrogen bonding; carboxylic acid; diamide; Hirshfeld surface analysis.

CCDC reference: 1453604

Supporting information: this article has supporting information at journals.iucr.org/e

The asymmetric unit of the title 2:1 co-crystal, $2C_8H_8O_2\cdot C_{14}H_{14}N_4O_2$, comprises an acid molecule in a general position and half a diamide molecule, the latter being located about a centre of inversion. In the acid, the carboxylic acid group is twisted out of the plane of the benzene ring to which it is attached [dihedral angle = 28.51 (8)°] and the carbonyl O atom and methyl group lie approximately to the same side of the molecule [hydroxy-O—C—C—C(H) torsion angle = −27.92 (17)°]. In the diamide, the central $C_4N_2O_2$ core is almost planar (r.m.s. deviation = 0.031 Å), and the pyridyl rings are perpendicular, lying to either side of the central plane [central residue/pyridyl dihedral angle = 88.60 (5)°]. In the molecular packing, three-molecule aggregates are formed *via* hydroxy-O—H···N(pyridyl) hydrogen bonds. These are connected into a supramolecular layer parallel to $(12\bar{2})$ *via* amide-N—H···O(carbonyl) hydrogen bonds, as well as methylene-C—H···O(amide) interactions. Significant π–π interactions occur between benzene/benzene, pyridyl/benzene and pyridyl/pyridyl rings within and between layers to consolidate the three-dimensional packing.

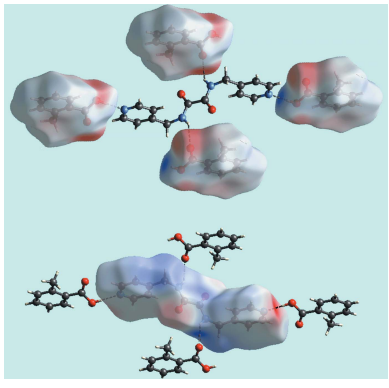

1. Chemical context

Multi-component crystals, incorporating co-crystals, salts and co-crystal salts, attract continuing interest for a wide variety of applications as this technology may be employed, for example, to provide additives to promote the growth of crystals, to stabilize unusual and unstable coformers, to generate new luminescent materials, to separate enantiomers, to facilitate absolute structure determination where the molecule of concern does not have a significant anomalous scatterer, *etc.* (Aakeröy, 2015; Tiekink, 2012). Arguably, the areas attracting most interest in this context are the applications of multi-component crystals in the pharmaceutical industry (Duggirala *et al.*, 2016). Controlled/designed crystallization of multi-component crystals requires reliable synthon formation between the various components and that, of course, is the challenge of crystal engineering, let alone engineering small aggregates within crystals (Tiekink, 2014).

Systematic work on synthon propensities in multi-component crystals have revealed that carboxylic acids have a great likelihood of forming hydroxy-O—H···N hydrogen bonds when co-crystallized with molecules with pyridyl residues (Shattock *et al.*, 2008). A plausible explanation for this reliability is the formation of a supporting carbonyl-O···H interaction involving the hydrogen atom adjacent to the pyridyl-

Table 1
Dihedral and torsion angles (°) for 2-methylbenzoic acid in the title co-crystal and in literature precedents.

Compound	$C_H-C-C-OH$	C_6/CO_2	CSD Refcode[b]	Reference
Parent compound	1.7 (2)	1.5 (5)	OTOLIC02	Thakur & Desiraju (2008)
1:1 Co-crystal with CF_1	7.5 (2)	8.04 (9)	WICZUF	Day *et al.* (2009)
1:1 Co-crystal with CF_2	4.25 (19)	4.02 (12)	EXIBOD	Ebenezer *et al.* (2011)
1:1 Co-crystal with CF_3	27.4 (3)	27.8 (2)	EXIZIR	Ebenezer *et al.* (2011)
1:1 Co-crystal with CF_4	23.0 (2)	23.86 (8)	CEKLEL	Wales *et al.* (2012)
Title co-crystal	−27.92 (18)	28.51 (8)	–	This work

Notes: (*a*) Refer to Scheme 2 for the chemical structures of coformers CF_1–CF_4. (*b*) Groom & Allen (2014).

nitrogen atom. Indeed, in the absence of competing hydrogen-bonding functionality, the resulting seven-membered {···HOCO···HCN} heterosynthon is formed in more than 98% of relevant crystal structures (Shattock *et al.*, 2008). Recent systematic work in this phenomenon relates to molecules shown in Scheme 1, where isomeric molecules with two pyridyl rings separated by a diamide residue have been co-crystallized with various carboxylic acids (Arman, Miller *et al.*, 2012; Arman *et al.*, 2013, Syed *et al.*, 2016; Jotani *et al.*, 2016). As a continuation of these studies, the title 2:1 co-crystal was isolated and characterized crystallographically and by Hirshfeld surface analysis.

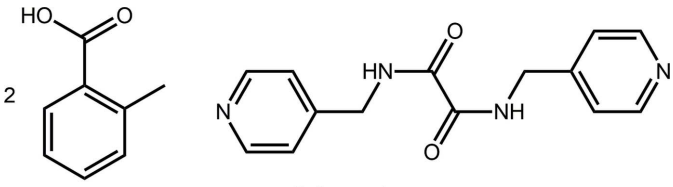

Scheme 1

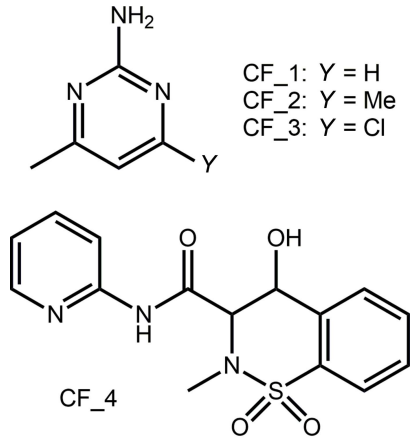

Scheme 2

2. Structural commentary

The title co-crystal, Fig. 1, was formed from the 1:1 co-crystallization of 2-methylbenzoic acid (hereafter, the acid) and *N*,*N*′-bis(pyridin-4-ylmethyl)ethanediamide (hereafter, the diamide) conducted in ethanol solution. The asymmetric unit comprises a full acid molecule in a general position and half a diamide molecule, located about a centre of inversion, so the co-crystal is formulated as a 2:1 acid:diamide co-crystal.

In the acid, the carboxylic acid group is twisted out of the plane of the benzene ring to which it is attached with the O3—C8—C9—C10 torsion angle being 150.23 (14)°, and, to a first approximation, with the carbonyl-O3 atom and methyl group lying to the same side of the molecule as indicated in the O2—C8—C9—C10 torsion angle of −27.92 (17)°. The structure of the parent acid and several co-crystals featuring coformers shown in Scheme 2 are available for comparison; data are collected in Table 1. The common feature of all structures is the relative orientation of the carbonyl-O and methyl groups. Twists in the acid molecules vary from almost co-planar to the situation found in the title co-crystal, with an even split of conformations amongst the six known co-crystal structures.

In the centrosymmetric diamide, the central $C_4N_2O_2$ core is essentially planar with an r.m.s. deviation (O1, N2, C6, C7 and symmetry equivalents) = 0.031 Å. This arrangement facilitates

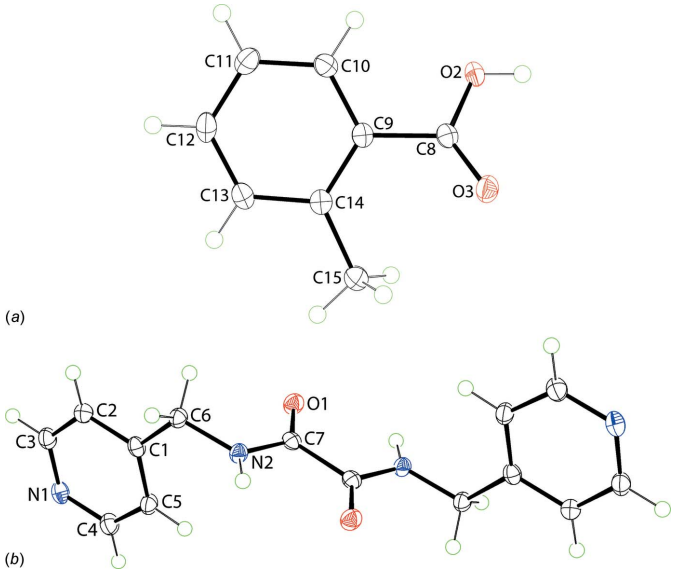

Figure 1
The molecular structures of the molecules comprising the title co-crystal showing the atom-labelling scheme and displacement ellipsoids at the 50% probability level: (*a*) 2-methylbenzoic acid and (*b*) *N*,*N*′-bis(pyridin-4-ylmethyl)ethanediamide; unlabelled atoms in the diamide are generated by the symmetry operation (−1 − *x*, 2 − *y*, 1 − *z*).

Table 2
Hydrogen-bond geometry (Å, °).

D—H···A	D—H	H···A	D···A	D—H···A
N2—H2N···O1^{i}	0.87 (1)	2.31 (1)	2.7100 (16)	108 (1)
O2—H2O···N1	0.85 (2)	1.79 (2)	2.6378 (16)	178 (2)
N2—H2N···O3^{ii}	0.87 (1)	2.17 (1)	2.8933 (15)	140 (1)
C6—H3B···O1^{iii}	0.99	2.48	3.3461 (18)	146

Symmetry codes: (i) $-x-1, -y+2, -z+1$; (ii) $-x, -y+1, -z+1$; (iii) $-x, -y+2, -z+1$.

the formation of an intramolecular amide-N—H···O(amide) hydrogen bond, Table 2. The pyridyl rings occupy positions on opposite sides of the central residue and project almost prime

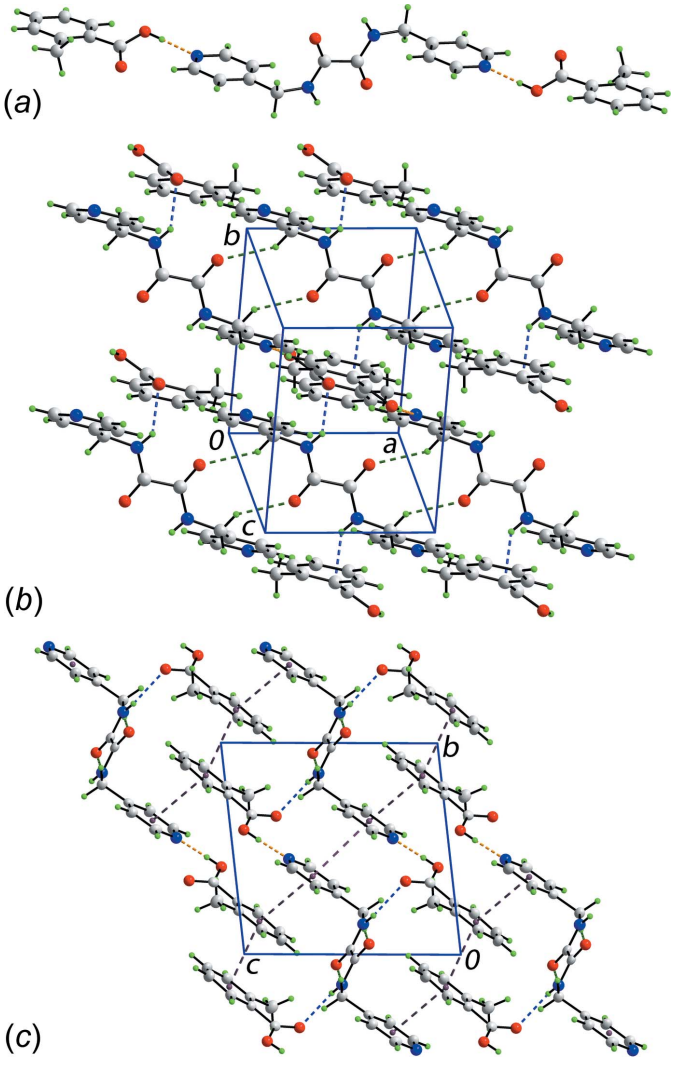

Figure 2
Molecular packing in the title co-crystal: (*a*) three-molecule aggregate sustained by hydroxy-O—H···N(pyridyl) hydrogen bonds, (*b*) supramolecular layers whereby the aggregates in (*a*) are connected by amide-N—H···O(carbonyl) and methylene-C—H···O(amide) interactions, and (*c*) a view of the unit-cell contents shown in projection down the *a* axis, highlighting the intra- and inter-layer π–π interactions to consolidate a three-dimensional architecture. The O—H···N, N—H···O, C—H···O and π–π interactions are shown as orange, blue, green and purple dashed lines, respectively.

to this with the central residue/pyridyl dihedral angle being 88.60 (5)°. The aforementioned structural features match literature precedents, *i.e.* the two polymorphic forms of the parent diamide and the diamide in co-crystals with carboxylic acids and in a salt with a carboxylate, Table 3. Finally, the central C—C bond length, considered long for a Csp^2—Csp^2 bond (Spek, 2009), matches the structural data included in Table 3; see Scheme 3 for chemical diagrams of coformers.

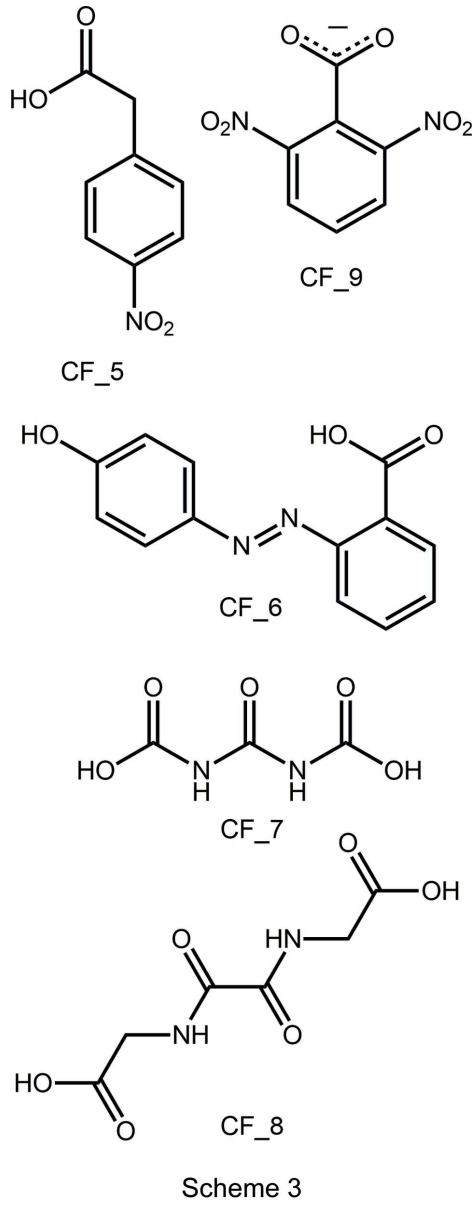

Scheme 3

3. Supramolecular features

The molecular packing of the title co-crystal is dominated by hydrogen bonding, detailed in Table 2. The acid is connected to the diamide *via* hydroxy-O—H···N(pyridyl) hydrogen bonds to form a three-molecule aggregate, Fig. 2*a*. The interacting residues are not co-planar with the dihedral angle between the pyridyl and three CO_2 groups being 25.67 (8)° so

Table 3
Selected geometric details (Å, °) for *N*,*N*′-bis(pyridin-4-ylmethyl)ethanediamide molecules and protonated forms[a].

Coformer	$C_4N_2O_2$/N-ring	C(═O)—C(═O)	Refcode[b]	Ref.
–[c,d]	74.90 (4)	1.532 (2)	CICYOD01	Lee (2010)
–[e]	68.83 (4); 70.89 (5)	1.541 (3)	CICYOD	Lee & Wang (2007)
	80.46 (5); 83.35 (6)	1.541 (3)		
CF_5[c,f]	87.37 (4)	1.534 (2)	NAXMEG	Arman, Kaulgud *et al.* (2012)
CF_6[c,f]	79.86 (4)	1.542 (2)	AJEZEV	Arman *et al.* (2009)
CF_7[g]	70.50 (4); 76.89 (4)	1.52 (2)	CAJRAH	Nguyen *et al.* (2001)
CF_8[c,g,h]	73.38 (11)	1.523 (7)	SEPSIP	Nguyen *et al.* (1998)
CF_8[c,g,i]	72.87 (9)	1.514 (5)	SEPSIP01	Nguyen *et al.* (2001)
CF_9[c,f]	75.83 (5)	1.543 (3)	TIPGUW	Arman *et al.* (2013)
2-Methylbenzoic acid	88.66 (4)	1.5356 (19)	–	This work

Notes: (*a*) Refer to Scheme 3 for the chemical structures of coformers, CF_5–CF_9; (*b*) Groom & Allen (2014); (*c*) molecule/dianion is centrosymmetric; (*d*) form I; (*e*) form II (two independent molecules); (*f*) 2:1 carboxylic acid/carboxylate diamide co-crystal/salt; (*g*) 1:1 dicarboxylic acid diamide co-crystal; (*h*) form I; (*i*) form II.

Table 4
π–π Interactions (Å, °).

Ring 1	Ring 2	Inter-centroid distance	Dihedral angle	Symmetry
N1,C1–C5	N1,C1–C5	3.5980 (8)	0	$-x, 1-y, 1-z$
N1,C1–C5	C9–C14	3.7833 (9)	4.63 (7)	$1-x, 1-y, -z$
C9–C14	C9–C14	3.8473 (8)	0	$-1-x, -y, -z$

that the carbonyl-O3···H3 distance is 2.60 Å. This suggests only a minor role for the putative seven-membered heterosynthon {···OCOH···NCH} mentioned in the *Chemical context* and is consistent with the significant hydrogen-bonding interaction involving the carbonyl-O3 atom to another residue. Indeed, the three-molecule aggregates are connected into a supramolecular layer parallel to $(12\overline{2})$ *via* amide-N—H···O(carbonyl) hydrogen bonds as well as methylene-C—H···O(amide) interactions, Fig. 2*b*. Within layers, π–π interactions occur between pyridyl rings, and between layers additional π–π interactions occur between pyridyl/benzene and benzene/benzene rings to consolidate the three-dimensional packing, Table 4 and Fig. 2*c*. Globally, the packing may be described as comprising alternating layers of aromatic rings and non-aromatic residues.

4. Analysis of the Hirshfeld surfaces

Crystal Explorer 3.1 (Wolff *et al.*, 2012) was used to generate Hirshfeld surfaces mapped over d_{norm}, d_e, electrostatic potential, shape-index and curvedness for the title 2:1 co-crystal. The electrostatic potentials were calculated using *TONTO* (Spackman *et al.*, 2008; Jayatilaka *et al.*, 2005) integrated with *Crystal Explorer*, using the experimentally determined geometry as the input. Further, the electrostatic potentials were mapped on Hirshfeld surfaces using the STO-3G basis set at Hartree–Fock theory over a range ±0.15 au. The contact distances d_i and d_e from the Hirshfeld surface to the nearest atom inside and outside, respectively, enabled the analysis of the intermolecular interactions through the mapping of d_{norm}. The combination of d_i and d_e in the form of a two-dimensional fingerprint plot (Rohl *et al.*, 2008) provides a summary of the intermolecular contacts.

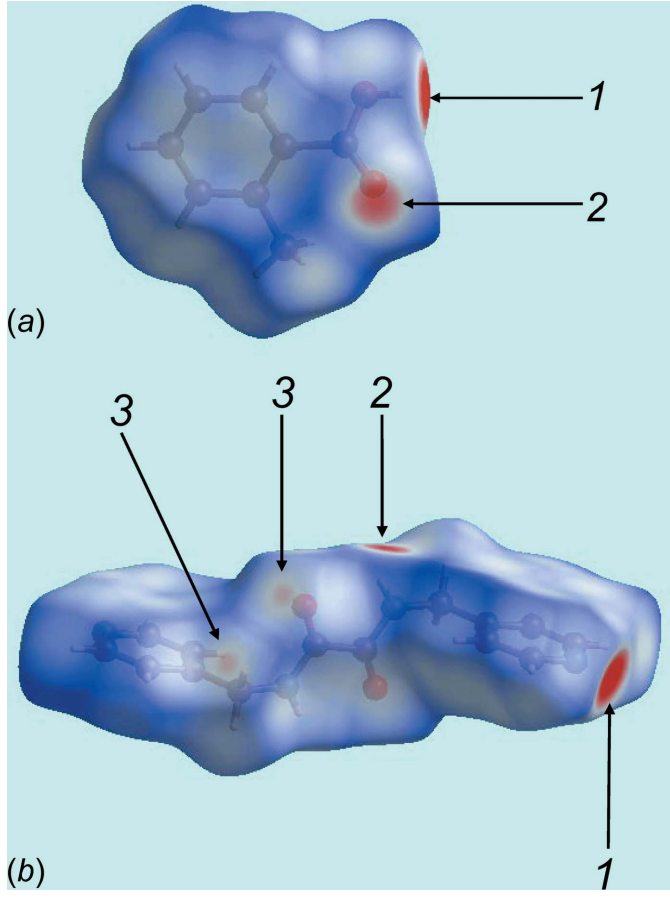

Figure 3
Views of the Hirshfeld surfaces mapped over d_{norm}: (*a*) acid and (*b*) diamide in the title 2:1 co-crystal. The contact points (red) are labelled to indicate the atoms participating in the intermolecular interactions.

Table 5
Major percentage contribution of the different intermolecular interactions to the Hirshfeld surfaces for the acid, diamide and 2:1 co-crystal.

Contact	Acid	Diamide	Co-crystal
H···H	48.7	45.2	49.9
O···H/H···O	20.6	25.6	21.3
C···H/H···C	16.7	12.0	15.9
N···H/H···N	3.8	8.9	2.7
C···C	5.9	6.4	6.6

The strong hydroxy-O—H···N(pyridyl) and amide-N—H···O(carbonyl) interactions between the acid and diamide molecules are visualized as bright-red spots at the respective donor and acceptor atoms on the Hirshfeld surfaces mapped over d_{norm}, and labelled as 1 and 2 in Fig. 3. The intermolecular methylene-C—H···O(amide) interactions appears as faint-red spots in Fig. 3*b*, marked with a '3'. The immediate environment about each molecule highlighting close contacts to the Hirshfeld surface by neighbouring molecules is shown in Fig. 4. The full fingerprint (FP) plots showing various crystal packing interactions in the acid, diamide and 2:1 co-crystal are shown in Fig. 5; the contributions from various contacts are listed in Table 5.

The prominent long spike at $d_e + d_i$ ~1.8 Å in the upper left (donor) region for the FP plot of the acid corresponds to H···N contacts and the spike at the same distance in the lower right (acceptor) region of the FP plot for the diamide are the result of hydroxy-O—H···N(pyridyl) interactions, Fig. 5*a* and *b*, respectively. However, these spikes are not apparent in the overall FP for the 2:1 co-crystal as they no longer contribute to the surface of the resultant aggregate, Fig. 5*c*. Pairs of somewhat blunted spikes corresponding to N···H/H···N contacts at $d_e + d_i \sim 2.9$ Å result from amide-N—H···O(carbonyl) interactions between the acid and diamide molecules are evident in the overall FP, Fig. 5*c*.

The O···H/H···O contacts, which make a significant contribution to the molecular packing, show different characteristic features in the respective delineated FP plots of the acid and diamide. For the acid, Fig. 5*a*, a long prominent spike at $d_e + d_i \sim 2.5$ Å in the acceptor region corresponds to a 6.6% contribution from H···O contacts to the Hirshfeld surface, and a short spike at $d_e + d_i \sim 2.15$ Å in the donor region with a 14.0% contribution. The reverse situation is observed for the diamide molecule wherein the FP plot, Fig. 5*b*, contains a long

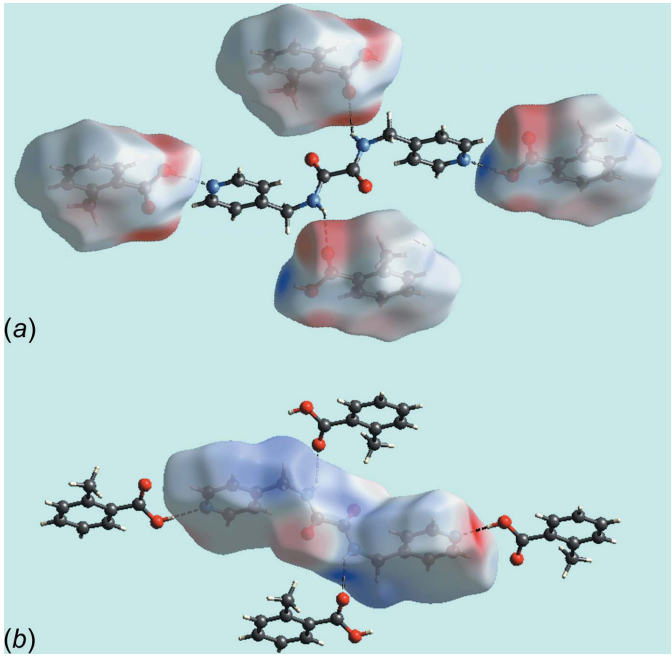

Figure 4
Hirshfeld surfaces mapped over d_{norm} showing hydrogen bonds with neighbouring molecules with the reference molecule being the (*a*) acid and (*b*) diamide.

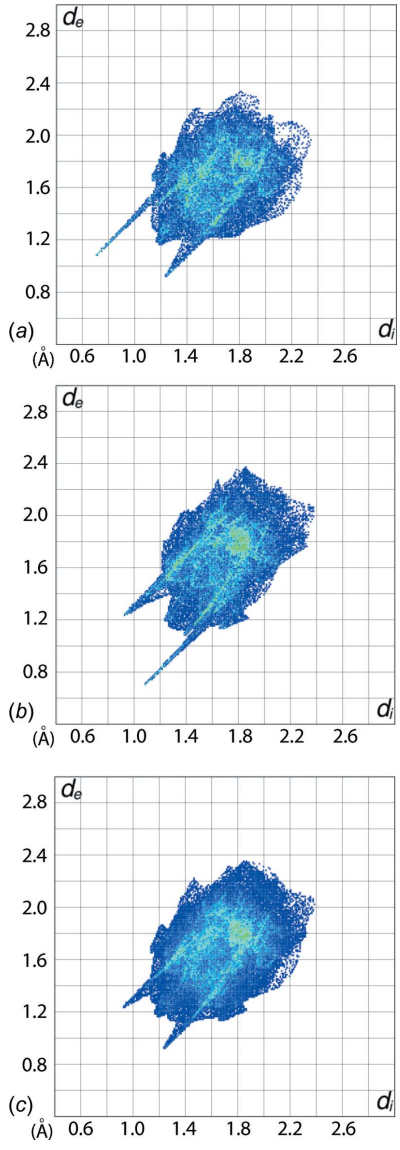

Figure 5
The two-dimensional fingerprint plots for the (*a*) acid, (*b*) diamide, and (*c*) overall 2:1 co-crystal.

Table 6
Enrichment ratios (ER) for the acid, diamide and co-crystal.

Interaction	Acid	Diamide	Co-crystal
H···H	1.02	0.97	1.02
O···H/H···O	1.22	1.46	1.30
C···C	2.30	3.60	2.55
C···H/H···C	0.75	0.66	0.71
N···H/H···N	1.06	1.20	0.84

prominent spike in the donor region and the short spike in the acceptor at the same $d_e + d_i$ distance, and with 10.7 and 14.9% contributions from O···H and H···O contacts, respectively.

FP plots for the co-crystal delineated into H···H, O···H/H···O, C···H/H···C, N···H/H···N and C···C are shown in Fig. 6*a*–*e*, respectively. The H···H contacts appear as asymmetrically scattered points covering a large region of the FP plot with a single broad peak at $d_e = d_i \sim 1.2$ Å for each of the co-crystal constituents, with percentage contributions of 48.7 and 45.7% for the acid and diamide molecules, respectively.

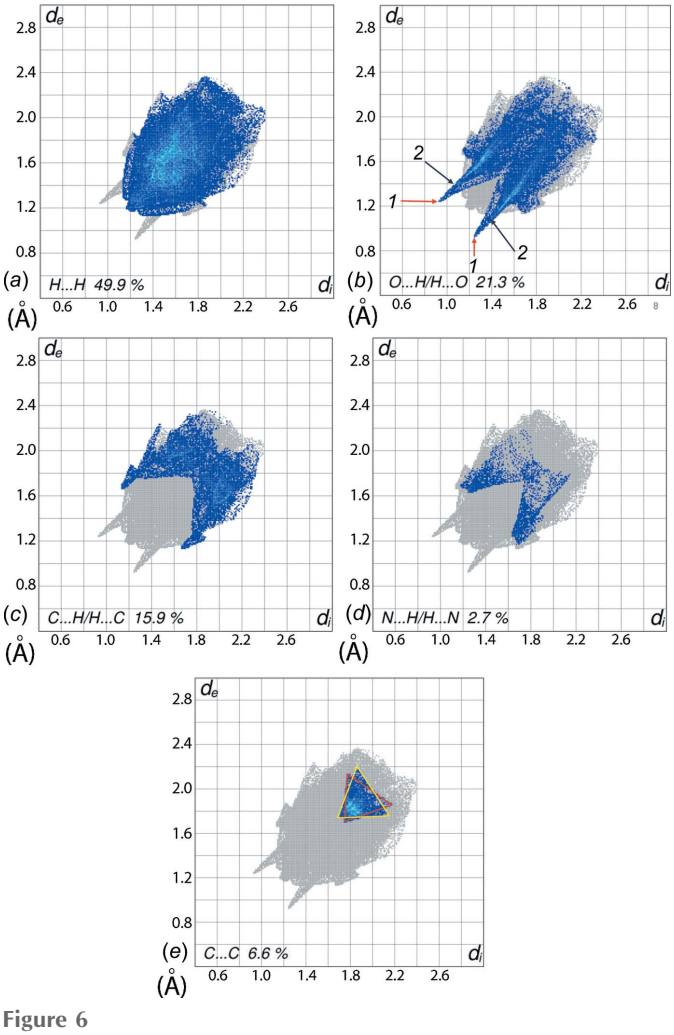

Figure 6
The two-dimensional fingerprint plot for the title 2:1 co-crystal showing contributions from different contacts: (*a*) H···H, (*b*) O···H/H···O, (*c*) C···H/H···C, (*d*) N···H/H···N, and (*e*) C···C.

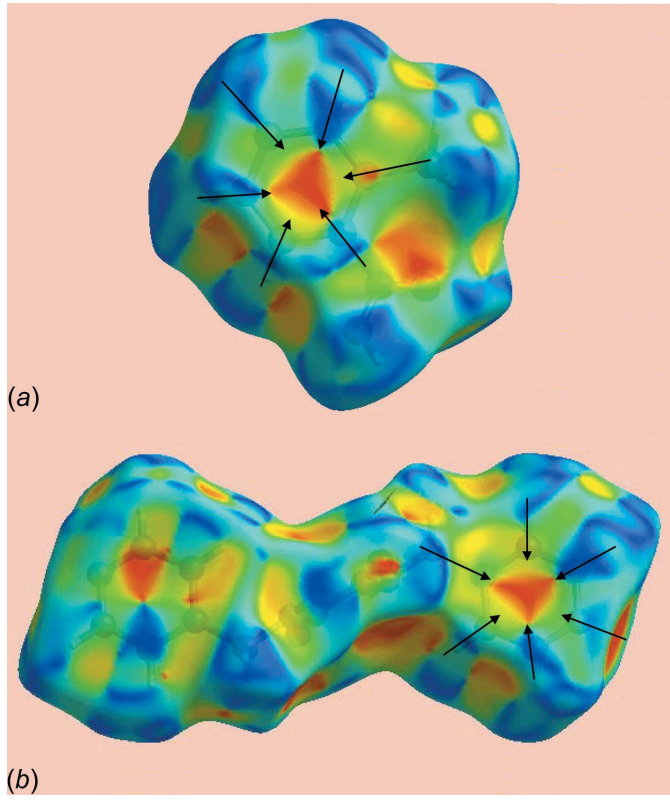

Figure 7
Hirshfeld surfaces mapped over the shape index for (*a*) the acid and (*b*) the diamide, highlighting the regions involved in π–π stacking interactions.

The overall 49.9% contribution to Hirshfeld surface of the co-crystal results in nearly symmetric through the superimposition of individual fingerprint plots, Fig. 6*a*.

The FP plot for O···H/H···O contacts, Fig. 6*b*, has two pairs of spikes superimposed in the (d_e, d_i) region with minimum $d_e + d_i$ distances $\sim$ 2.2 and 2.5 Å. These correspond to a 21.3% contribution to the Hirshfeld surface, and reflect the presence of intermolecular N—H···O and C—H···O interactions, identified with labels 1 and 2 in Fig. 6*b*. The 15.9% contribution from the C···H/H···C contacts to the Hirshfeld surface results in a symmetric pair of wings, Fig. 6*c*. The FP plot corresponding to C···C contacts, Fig. 6*e*, in the (d_e, d_i) region between 1.7 to 2.2 Å appears as the two distinct, overlapping triangles identified with red and yellow boundaries in Fig. 6*e*, and shows two types of π–π stacking interactions: one between dissimilar rings (pyridyl and benzene) and the other between symmetry-related rings (benzene and benzene, and pyridyl and pyridyl). The presence of these π–π stacking interactions is also indicated by the appearance of red and blue triangles on the shape-indexed surfaces identified with arrows in the images of Fig. 7, and in the flat regions on the Hirshfeld surfaces mapped with curvedness in Fig. 8.

The intermolecular interactions were further assessed by using the enrichment ratio, ER (Jelsch *et al.*, 2014). This is a relatively new descriptor and is based on Hirshfeld surface analysis. The ER for the co-crystal together with those for the acid and diamide molecules are listed in Table 6. The largest

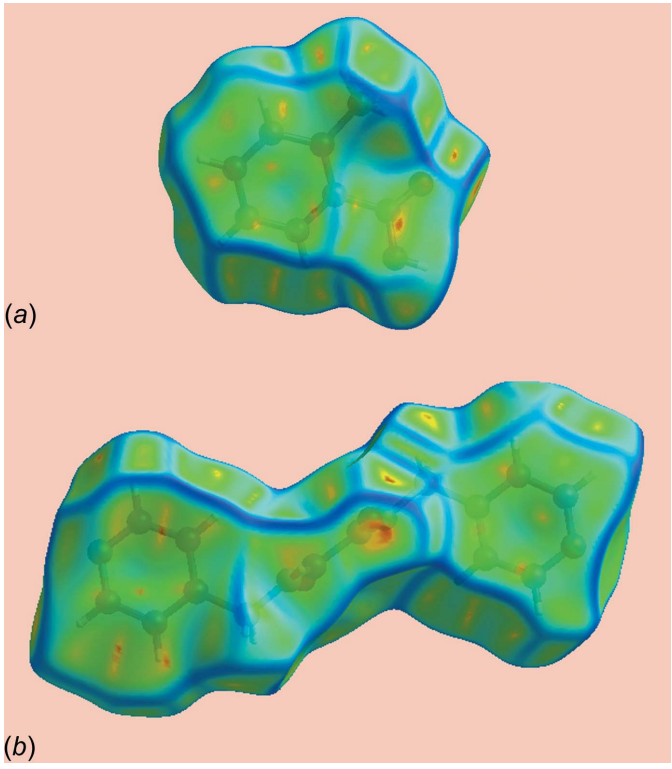

Figure 8
Hirshfeld surfaces mapped over curvedness for (*a*) the acid and (*b*) the diamide, highlighting the regions involved in π–π stacking interactions.

Table 7
Experimental details.

Crystal data	
Chemical formula	$C_{14}H_{14}N_4O_2{\cdot}2C_8H_8O_2$
M_r	542.58
Crystal system, space group	Triclinic, $P\overline{1}$
Temperature (K)	100
a, b, c (Å)	6.8948 (5), 9.7219 (5), 9.9621 (7)
α, β, γ (°)	82.971 (5), 81.638 (6), 85.686 (5)
V (Å^3)	654.58 (8)
Z	1
Radiation type	Mo $K\alpha$
μ (mm^{-1})	0.10
Crystal size (mm)	0.21 × 0.15 × 0.10
Data collection	
Diffractometer	Agilent Technologies SuperNova Dual diffractometer with an Atlas detector
Absorption correction	Multi-scan (*CrysAlis PRO*; Agilent, 2014)
T_{min}, T_{max}	0.580, 1.000
No. of measured, independent and observed [$I > 2\sigma(I)$] reflections	15067, 2993, 2358
R_{int}	0.044
(sin $\theta/\lambda)_{max}$ (Å^{-1})	0.650
Refinement	
$R[F^2 > 2\sigma(F^2)]$, $wR(F^2)$, S	0.041, 0.106, 1.06
No. of reflections	2993
No. of parameters	188
No. of restraints	2
$\Delta\rho_{max}$, $\Delta\rho_{min}$ (e Å^{-3})	0.34, −0.23

Computer programs: *CrysAlis PRO* (Agilent, 2014), *SHELXS97* (Sheldrick, 2008), *SHELXL2014* (Sheldrick, 2015), *ORTEP-3 for Windows* (Farrugia, 2012), *DIAMOND* (Brandenburg, 2006) and *publCIF* (Westrip, 2010).

contribution to the Hirshfeld surfaces are from H···H contacts, Table 5, and their respective ER values are close to unity. This shows that the contribution from dispersive forces are significant in the molecule packing of the title 2:1 co-crystal, in contrast to that observed in a related, recently published structure, namely, the salt [2-({[(pyridin-1-ium-2-ylmethyl)carbamoyl]formamido}methyl)-pyridin-1-ium][3,5-dicarboxybenzoate], *i.e.* containing the diprotonated form of the isomeric 2-pyridyl-containing diamide (Syed *et al.*, 2016). In the latter, O···H/H···O contacts make the greatest contribution to the crystal packing. It is the presence of different substituents in the benzene ring in the acid molecule in the co-crystal, *i.e.* methyl, as opposed to carboxylic acid/carboxylate groups in the salt, that provides an explanation for this difference. The ER value for O···H/H···O contacts, *i.e.* 1.30, shows the propensity to form hydroxy-O—H···N(pyridyl) and amide-N—H···O(carbonyl) hydrogen bonds as well as methylene-C—H···O(amide) interactions. The formation of extensive π–π interactions is reflected in the relatively high ER values corresponding/related to C···C contacts, Table 6. The absence of C—H···π and related interactions is reflected in low ER values, *i.e.* < 0.8. Conversely, the N···H/H···N contacts in a crystal having ER values equal to greater than or equal to unity for the acid/diamide molecules reduces to 0.84 in the 2:1 co-crystal, indicating a reduced likelihood of formation once the co-crystal is stabilized by other interactions. The enrichment ratios for other contacts are of low significance as they are derived from less important interactions which have small contributions to Hirshfeld surfaces.

5. Database survey

As mentioned in the *Chemical context*, the diamide in the title 2:1 co-crystal and isomeric forms have attracted considerable interest in the crystal engineering community no doubt owing to the variable functional groups and conformational flexibility. Indeed, the diamide in the title co-crystal featured in early studies of halogen I···N halogen bonding (Goroff *et al.*, 2005). Over and above these investigations, the role of the diamide in coordination chemistry has also been studied. Bidentate bridging is the prominent coordination mode observed in both neutral, *e.g.* $[HgI_2(\text{diamide})]_n$ (Zeng *et al.*, 2008) and charged, *e.g.* polymeric $[Ag(\text{diamide})NO_3]_n$ (Schauer *et al.*, 1998) and oligiomeric $\{[Ph_2PCH_2PPh_2Au_2(\text{diamide})]_2(ClO_4)_4(EtOEt)_4\}$ (Tzeng *et al.*, 2006), species.

6. Synthesis and crystallization

The diamide (0.2 g), prepared in accord with the literature procedure (Schauer *et al.*, 1997), in ethanol (10 ml) was added to a ethanol solution (10 ml) of 2-methylbenzoic acid (Merck, 0.1 g). The mixture was stirred for 1 h at room temperature after which a white precipitate was deposited. The solution was filtered by vacuum suction, and the filtrate was then left to

stand under ambient conditions, yielding colourless prisms after 2 weeks.

7. Refinement

Crystal data, data collection and structure refinement details are summarized in Table 7. The carbon-bound H-atoms were placed in calculated positions (C—H = 0.95–0.99 Å) and were included in the refinement in the riding-model approximation, with U_{iso}(H) set to 1.2U_{eq}(C). The oxygen- and nitrogen-bound H-atoms were located in a difference Fourier map but were refined with distance restraints of O—H = 0.84±0.01 Å and N—H = 0.88±0.01 Å, and with U_{iso}(H) set to 1.5U_{eq}(O) and 1.2U_{eq}(N).

Acknowledgements

The authors thank the Exploratory Research Grant Scheme (ER008-2013A) for support.

References

Aakeröy, C. (2015). *Acta Cryst.* B**71**, 387–391.
Agilent (2014). *CrysAlis PRO*. Agilent Technologies Inc., Santa Clara, CA, USA.
Arman, H. D., Kaulgud, T., Miller, T., Poplaukhin, P. & Tiekink, E. R. T. (2012). *J. Chem. Crystallogr.* **42**, 673–679.
Arman, H. D., Kaulgud, T., Miller, T. & Tiekink, E. R. T. (2013). *Z. Kristallogr*. **229**, 295–302.
Arman, H. D., Miller, T., Poplaukhin, P. & Tiekink, E. R. T. (2009). *Acta Cryst.* E**65**, o3178–o3179.
Arman, H. D., Miller, T. & Tiekink, E. R. T. (2012). *Z. Kristallogr*. **227**, 825–830.
Brandenburg, K. (2006). *DIAMOND*. Crystal Impact GbR, Bonn, Germany.
Day, G. M., Cooper, T. G., Cruz-Cabeza, A. J., Hejczyk, K. E., Ammon, H. L., Boerrigter, S. X. M., Tan, J. S., Della Valle, R. G., Venuti, E., Jose, J., Gadre, S. R., Desiraju, G. R., Thakur, T. S., van Eijck, B. P., Facelli, J. C., Bazterra, V. E., Ferraro, M. B., Hofmann, D. W. M., Neumann, M. A., Leusen, F. J. J., Kendrick, J., Price, S. L., Misquitta, A. J., Karamertzanis, P. G., Welch, G. W. A., Scheraga, H. A., Arnautova, Y. A., Schmidt, M. U., van de Streek, J., Wolf, A. K. & Schweizer, B. (2009). *Acta Cryst.* B**65**, 107–125.
Duggirala, N. K., Perry, M. L., Almarsson, Ö. & Zaworotko, M. J. (2016). *Chem. Commun.* **52**, 640–655.
Ebenezer, S., Muthiah, P. T. & Butcher, R. J. (2011). *Cryst. Growth Des.* **11**, 3579–3592.
Farrugia, L. J. (2012). *J. Appl. Cryst.* **45**, 849–854.
Goroff, N. S., Curtis, S. M., Webb, J. A., Fowler, F. W. & Lauher, J. W. (2005). *Org. Lett.* **7**, 1891–1893.
Groom, C. R. & Allen, F. H. (2014). *Angew. Chem. Int. Ed.* **53**, 662–671.
Jayatilaka, D., Grimwood, D. J., Lee, A., Lemay, A., Russel, A. J., Taylor, C., Wolff, S. K., Cassam-Chenai, P. & Whitton, A. (2005). *TONTO – A System for Computational Chemistry*. Available at: http://hirshfeldsurface.net/
Jelsch, C., Ejsmont, K. & Huder, L. (2014). *IUCrJ*, **1**, 119–128.
Jotani, M. M., Syed, S., Halim, S. N. A. & Tiekink, E. R. T. (2016). *Acta Cryst.* E**72**, 241–248.
Lee, G.-H. (2010). *Acta Cryst.* C**66**, o241–o244.
Lee, G.-H. & Wang, H.-T. (2007). *Acta Cryst.* C**63**, m216–m219.
Nguyen, T. L., Fowler, F. W. & Lauher, J. W. (2001). *J. Am. Chem. Soc.* **123**, 11057–11064.
Nguyen, T. L., Scott, A., Dinkelmeyer, B., Fowler, F. W. & Lauher, J. W. (1998). *New J. Chem*. **22**, 129–135.
Rohl, A. L., Moret, M., Kaminsky, W., Claborn, K., McKinnon, J. J. & Kahr, B. (2008). *Cryst. Growth Des.* **8**, 4517–4525.
Schauer, C. L., Matwey, E., Fowler, F. W. & Lauher, J. W. (1997). *J. Am. Chem. Soc.* **119**, 10245–10246.
Schauer, C. L., Matwey, E., Fowler, F. W. & Lauher, J. W. (1998). *Cryst. Eng.* **1**, 213–223.
Shattock, T., Arora, K. K., Vishweshwar, P. & Zaworotko, M. J. (2008). *Cryst. Growth Des.* **8**, 4533–4545.
Sheldrick, G. M. (2008). *Acta Cryst.* A**64**, 112–122.
Sheldrick, G. M. (2015). *Acta Cryst.* C**71**, 3–8.
Spackman, M. A., McKinnon, J. J. & Jayatilaka, D. (2008). *CrystEngComm*, **10**, 377–388.
Spek, A. L. (2009). *Acta Cryst.* D**65**, 148–155.
Syed, S., Halim, S. N. A., Jotani, M. M. & Tiekink, E. R. T. (2016). *Acta Cryst.* E**72**, 76–82.
Thakur, T. S. & Desiraju, G. R. (2008). *Cryst. Growth Des.* **8**, 4031–4044.
Tiekink, E. R. T. (2012). *Crystal engineering. In Supramolecular Chemistry: from Molecules to Nanomaterials*, edited by J. W. Steed & P. A. Gale, pp. 2791–2828. Chichester: John Wiley & Sons Ltd.
Tiekink, E. R. T. (2014). *Chem. Commun.* **50**, 11079–11082.
Tzeng, B.-C., Yeh, H.-T., Wu, Y.-L., Kuo, J. H., Lee, G.-H. & Peng, S.-M. (2006). *Inorg. Chem.* **45**, 591–598.
Wales, C., Thomas, L. H. & Wilson, C. C. (2012). *CrystEngComm*, **14**, 7264–7274.
Westrip, S. P. (2010). *J. Appl. Cryst.* **43**, 920–925.
Wolff, S. K., Grimwood, D. J., McKinnon, J. J., Turner, M. J., Jayatilaka, D. & Spackman, M. A. (2012). *Crystal Explorer*. The University of Western Australia.
Zeng, Q., Li, M., Wu, D., Lei, S., Liu, C., Piao, L., Yang, Y., An, S. & Wang, C. (2008). *Cryst. Growth Des.* **8**, 869–876.

supporting information

Acta Cryst. (2016). E**72**, 391-398 [doi:10.1107/S2056989016002735]

A 2:1 co-crystal of 2-methylbenzoic acid and *N*,*N*′-bis(pyridin-4-ylmethyl)-ethanediamide: crystal structure and Hirshfeld surface analysis

Sabrina Syed, Mukesh M. Jotani, Siti Nadiah Abdul Halim and Edward R. T. Tiekink

Computing details

Data collection: *CrysAlis PRO* (Agilent, 2014); cell refinement: *CrysAlis PRO* (Agilent, 2014); data reduction: *CrysAlis PRO* (Agilent, 2014); program(s) used to solve structure: *SHELXS97* (Sheldrick, 2008); program(s) used to refine structure: *SHELXL2014* (Sheldrick, 2015); molecular graphics: *ORTEP-3 for Windows* (Farrugia, 2012) and *DIAMOND* (Brandenburg, 2006); software used to prepare material for publication: *publCIF* (Westrip, 2010).

2-Methylbenzoic acid–\ *N*,*N*′-bis(pyridin-4-ylmethyl)ethanediamide (2/1)

Crystal data

$C_{14}H_{14}N_4O_2{\cdot}2C_8H_8O_2$
M_r = 542.58
Triclinic, $P\overline{1}$
a = 6.8948 (5) Å
b = 9.7219 (5) Å
c = 9.9621 (7) Å
α = 82.971 (5)°
β = 81.638 (6)°
γ = 85.686 (5)°
V = 654.58 (8) Å^3
Z = 1
$F(000)$ = 286
D_x = 1.376 Mg m^{-3}
Mo $K\alpha$ radiation, λ = 0.71073 Å
Cell parameters from 3840 reflections
θ = 3.5–30.0°
μ = 0.10 mm^{-1}
T = 100 K
Prism, colourless
0.21 × 0.15 × 0.10 mm

Data collection

Agilent Technologies SuperNova Dual diffractometer with an Atlas detector
Radiation source: SuperNova (Mo) X-ray Source
Mirror monochromator
Detector resolution: 10.4041 pixels mm^{-1}
ω scan
Absorption correction: multi-scan (*CrysAlis PRO*; Agilent, 2014)
T_{min} = 0.580, T_{max} = 1.000
15067 measured reflections
2993 independent reflections
2358 reflections with $I > 2\sigma(I)$
R_{int} = 0.044
θ_{max} = 27.5°, θ_{min} = 3.0°
h = −8→8
k = −12→12
l = −12→12

Refinement

Refinement on F^2
Least-squares matrix: full
$R[F^2 > 2\sigma(F^2)]$ = 0.041
$wR(F^2)$ = 0.106
S = 1.06
2993 reflections
188 parameters
2 restraints
Hydrogen site location: mixed
$w = 1/[\sigma^2(F_o^2) + (0.0434P)^2 + 0.2225P]$ where $P = (F_o^2 + 2F_c^2)/3$
$(\Delta/\sigma)_{max} < 0.001$
$\Delta\rho_{max}$ = 0.34 e Å^{-3}
$\Delta\rho_{min}$ = −0.23 e Å^{-3}

Special details

Geometry. All esds (except the esd in the dihedral angle between two l.s. planes) are estimated using the full covariance matrix. The cell esds are taken into account individually in the estimation of esds in distances, angles and torsion angles; correlations between esds in cell parameters are only used when they are defined by crystal symmetry. An approximate (isotropic) treatment of cell esds is used for estimating esds involving l.s. planes.

Fractional atomic coordinates and isotropic or equivalent isotropic displacement parameters (Å²)

	x	*y*	*z*	U_{iso}*/U_{eq}
O1	−0.26845 (15)	1.04906 (10)	0.41903 (10)	0.0202 (2)
N1	0.10595 (19)	0.54943 (12)	0.25502 (12)	0.0194 (3)
N2	−0.34990 (18)	0.85635 (11)	0.56442 (12)	0.0157 (3)
H2N	−0.4483 (18)	0.8165 (15)	0.6161 (14)	0.019*
C1	−0.0650 (2)	0.71369 (13)	0.45691 (14)	0.0159 (3)
C2	0.1324 (2)	0.66915 (14)	0.44690 (15)	0.0183 (3)
H2	0.2123	0.6945	0.5089	0.022*
C3	0.2113 (2)	0.58766 (14)	0.34574 (15)	0.0197 (3)
H3	0.3461	0.5574	0.3403	0.024*
C4	−0.0837 (2)	0.59250 (14)	0.26467 (15)	0.0205 (3)
H4	−0.1600	0.5661	0.2009	0.025*
C5	−0.1746 (2)	0.67411 (14)	0.36357 (15)	0.0182 (3)
H5	−0.3100	0.7024	0.3672	0.022*
C6	−0.1494 (2)	0.80107 (14)	0.57005 (14)	0.0165 (3)
H3A	−0.1442	0.7438	0.6589	0.020*
H3B	−0.0648	0.8796	0.5668	0.020*
C7	−0.3901 (2)	0.97768 (13)	0.49211 (14)	0.0154 (3)
O2	0.30435 (15)	0.41238 (10)	0.06130 (11)	0.0200 (2)
H2O	0.242 (2)	0.4581 (16)	0.1233 (15)	0.030*
O3	0.50558 (15)	0.34690 (10)	0.21737 (10)	0.0210 (2)
C8	0.4571 (2)	0.33987 (13)	0.10547 (14)	0.0160 (3)
C9	0.5600 (2)	0.24530 (13)	0.00615 (14)	0.0157 (3)
C10	0.4507 (2)	0.19550 (14)	−0.08313 (15)	0.0183 (3)
H10	0.3160	0.2250	−0.0817	0.022*
C11	0.5355 (2)	0.10374 (14)	−0.17385 (15)	0.0222 (3)
H11	0.4586	0.0672	−0.2314	0.027*
C12	0.7337 (2)	0.06622 (14)	−0.17932 (15)	0.0220 (3)
H12	0.7947	0.0059	−0.2432	0.026*
C13	0.8436 (2)	0.11621 (14)	−0.09211 (15)	0.0195 (3)
H13	0.9800	0.0904	−0.0983	0.023*
C14	0.7595 (2)	0.20349 (13)	0.00468 (14)	0.0166 (3)
C15	0.8858 (2)	0.24942 (15)	0.09983 (16)	0.0225 (3)
H15A	0.8762	0.3510	0.0945	0.034*
H15B	1.0226	0.2173	0.0735	0.034*
H15C	0.8409	0.2100	0.1935	0.034*

Atomic displacement parameters (Å²)

	U^{11}	U^{22}	U^{33}	U^{12}	U^{13}	U^{23}
O1	0.0158 (5)	0.0209 (5)	0.0229 (6)	−0.0017 (4)	−0.0010 (4)	−0.0004 (4)
N1	0.0224 (7)	0.0166 (6)	0.0179 (6)	0.0030 (5)	0.0001 (5)	−0.0027 (5)
N2	0.0132 (6)	0.0170 (6)	0.0166 (6)	0.0005 (4)	−0.0005 (5)	−0.0031 (4)
C1	0.0179 (7)	0.0129 (6)	0.0155 (7)	−0.0004 (5)	0.0001 (6)	0.0004 (5)
C2	0.0170 (7)	0.0173 (6)	0.0208 (7)	−0.0004 (5)	−0.0025 (6)	−0.0029 (5)
C3	0.0170 (7)	0.0164 (6)	0.0243 (8)	0.0011 (5)	0.0006 (6)	−0.0018 (6)
C4	0.0238 (8)	0.0190 (7)	0.0190 (7)	0.0025 (6)	−0.0048 (6)	−0.0037 (6)
C5	0.0160 (7)	0.0185 (7)	0.0199 (7)	0.0031 (5)	−0.0028 (6)	−0.0039 (5)
C6	0.0150 (7)	0.0176 (6)	0.0170 (7)	0.0011 (5)	−0.0021 (6)	−0.0035 (5)
C7	0.0176 (8)	0.0158 (6)	0.0137 (7)	−0.0006 (5)	−0.0019 (6)	−0.0058 (5)
O2	0.0177 (6)	0.0225 (5)	0.0196 (5)	0.0044 (4)	−0.0008 (4)	−0.0067 (4)
O3	0.0239 (6)	0.0232 (5)	0.0156 (5)	0.0019 (4)	−0.0012 (4)	−0.0042 (4)
C8	0.0154 (7)	0.0151 (6)	0.0163 (7)	−0.0020 (5)	0.0015 (6)	−0.0005 (5)
C9	0.0174 (7)	0.0144 (6)	0.0140 (7)	−0.0017 (5)	0.0009 (6)	0.0001 (5)
C10	0.0166 (7)	0.0197 (7)	0.0180 (7)	0.0005 (5)	−0.0023 (6)	−0.0008 (5)
C11	0.0283 (9)	0.0211 (7)	0.0185 (8)	−0.0015 (6)	−0.0062 (6)	−0.0039 (6)
C12	0.0296 (9)	0.0182 (7)	0.0172 (7)	0.0046 (6)	−0.0005 (6)	−0.0045 (6)
C13	0.0198 (8)	0.0186 (7)	0.0183 (7)	0.0028 (6)	0.0004 (6)	−0.0008 (5)
C14	0.0185 (7)	0.0140 (6)	0.0163 (7)	−0.0021 (5)	0.0000 (6)	0.0001 (5)
C15	0.0173 (8)	0.0259 (7)	0.0251 (8)	−0.0003 (6)	−0.0024 (6)	−0.0075 (6)

Geometric parameters (Å, º)

O1—C7	1.2252 (17)	O2—C8	1.3217 (17)
N1—C4	1.3364 (19)	O2—H2O	0.853 (9)
N1—C3	1.3401 (19)	O3—C8	1.2205 (17)
N2—C7	1.3371 (17)	C8—C9	1.4994 (18)
N2—C6	1.4510 (18)	C9—C10	1.396 (2)
N2—H2N	0.874 (9)	C9—C14	1.403 (2)
C1—C5	1.385 (2)	C10—C11	1.385 (2)
C1—C2	1.390 (2)	C10—H10	0.9500
C1—C6	1.5166 (18)	C11—C12	1.383 (2)
C2—C3	1.3820 (19)	C11—H11	0.9500
C2—H2	0.9500	C12—C13	1.384 (2)
C3—H3	0.9500	C12—H12	0.9500
C4—C5	1.3892 (19)	C13—C14	1.3964 (19)
C4—H4	0.9500	C13—H13	0.9500
C5—H5	0.9500	C14—C15	1.503 (2)
C6—H3A	0.9900	C15—H15A	0.9800
C6—H3B	0.9900	C15—H15B	0.9800
C7—C7^{i}	1.536 (3)	C15—H15C	0.9800
C4—N1—C3	117.67 (12)	C8—O2—H2O	110.8 (13)
C7—N2—C6	121.54 (12)	O3—C8—O2	123.13 (12)
C7—N2—H2N	117.2 (11)	O3—C8—C9	123.68 (13)

C6—N2—H2N	120.9 (11)	O2—C8—C9	113.16 (12)
C5—C1—C2	117.97 (13)	C10—C9—C14	120.20 (12)
C5—C1—C6	123.56 (13)	C10—C9—C8	118.28 (13)
C2—C1—C6	118.47 (13)	C14—C9—C8	121.48 (12)
C3—C2—C1	119.31 (14)	C11—C10—C9	121.07 (14)
C3—C2—H2	120.3	C11—C10—H10	119.5
C1—C2—H2	120.3	C9—C10—H10	119.5
N1—C3—C2	122.93 (14)	C12—C11—C10	118.97 (14)
N1—C3—H3	118.5	C12—C11—H11	120.5
C2—C3—H3	118.5	C10—C11—H11	120.5
N1—C4—C5	123.05 (14)	C11—C12—C13	120.28 (13)
N1—C4—H4	118.5	C11—C12—H12	119.9
C5—C4—H4	118.5	C13—C12—H12	119.9
C1—C5—C4	119.07 (13)	C12—C13—C14	121.79 (14)
C1—C5—H5	120.5	C12—C13—H13	119.1
C4—C5—H5	120.5	C14—C13—H13	119.1
N2—C6—C1	115.06 (12)	C13—C14—C9	117.56 (13)
N2—C6—H3A	108.5	C13—C14—C15	119.00 (13)
C1—C6—H3A	108.5	C9—C14—C15	123.43 (12)
N2—C6—H3B	108.5	C14—C15—H15A	109.5
C1—C6—H3B	108.5	C14—C15—H15B	109.5
H3A—C6—H3B	107.5	H15A—C15—H15B	109.5
O1—C7—N2	125.26 (13)	C14—C15—H15C	109.5
O1—C7—C7^{i}	121.45 (15)	H15A—C15—H15C	109.5
N2—C7—C7^{i}	113.29 (15)	H15B—C15—H15C	109.5

C5—C1—C2—C3	−0.2 (2)	O2—C8—C9—C10	−27.92 (17)
C6—C1—C2—C3	179.02 (12)	O3—C8—C9—C14	−27.8 (2)
C4—N1—C3—C2	−0.3 (2)	O2—C8—C9—C14	154.08 (12)
C1—C2—C3—N1	0.4 (2)	C14—C9—C10—C11	0.4 (2)
C3—N1—C4—C5	0.0 (2)	C8—C9—C10—C11	−177.60 (12)
C2—C1—C5—C4	−0.1 (2)	C9—C10—C11—C12	−2.8 (2)
C6—C1—C5—C4	−179.24 (12)	C10—C11—C12—C13	2.1 (2)
N1—C4—C5—C1	0.2 (2)	C11—C12—C13—C14	0.9 (2)
C7—N2—C6—C1	−87.65 (15)	C12—C13—C14—C9	−3.3 (2)
C5—C1—C6—N2	−7.47 (19)	C12—C13—C14—C15	177.62 (13)
C2—C1—C6—N2	173.38 (12)	C10—C9—C14—C13	2.56 (19)
C6—N2—C7—O1	4.4 (2)	C8—C9—C14—C13	−179.48 (12)
C6—N2—C7—C7^{i}	−175.86 (13)	C10—C9—C14—C15	−178.36 (13)
O3—C8—C9—C10	150.23 (14)	C8—C9—C14—C15	−0.4 (2)

Symmetry code: (i) −*x*−1, −*y*+2, −*z*+1.

Hydrogen-bond geometry (Å, º)

D—H···*A*	*D*—H	H···*A*	*D*···*A*	*D*—H···*A*
N2—H2*N*···O1^{i}	0.87 (1)	2.31 (1)	2.7100 (16)	108 (1)
O2—H2*O*···N1	0.85 (2)	1.79 (2)	2.6378 (16)	178 (2)

N2—H2*N*···O3^{ii}	0.87 (1)	2.17 (1)	2.8933 (15)	140 (1)
C6—H3*B*···O1^{iii}	0.99	2.48	3.3461 (18)	146

Symmetry codes: (i) −*x*−1, −*y*+2, −*z*+1; (ii) −*x*, −*y*+1, −*z*+1; (iii) −*x*, −*y*+2, −*z*+1.